Available online at www.sciencedirect.com

ScienceDirect

Ceramics International 40 (2014) 1835–1841

CERAMICS INTERNATIONAL

www.elsevier.com/locate/ceramint

# Preparation of lithium niobate particles via reactive molten salt synthesis method

Ali Reza Kamali*, Derek J. Fray

*Department of Materials Science and Metallurgy, University of Cambridge, Pembroke Street, Cambridge CB2 3QZ, UK*

Received 1 January 2013; received in revised form 29 June 2013; accepted 17 July 2013
Available online 3 August 2013

## Abstract

Lithium niobate ($LiNbO_3$, LN) is one of the key materials for optical based technologies. In this paper, we report an effective, simple, cheap and very fast molten salt method for gram-scale synthesis of single-crystalline LN particles in which a mixture of $Nb_2O_5$–LiCl is heat treated at a temperature above the melting point of LiCl for few minutes. The product consisted of LN and other Li–Nb–O phases when the mixture was heated in air. In contrast, single-phase LN was synthesised by heating the mixture in a humid argon flow. In this process, the molten salt acts as both the reaction medium and the Li-source. Synthesised LN was characterised by X-ray diffraction, scanning electron microscopy, transmission electron microscopy, differential scanning calorimetry, and Raman spectroscopy. The mechanism of the process is also discussed.

*Keywords:* Lithium niobate; Lithium chloride; Molten salt; Crystal growth

## 1. Introduction

Considerable interest exists in lithium-metal-oxides due to their many industrial and academic applications. Particularly, LN is a key material for ferroelectric, pyroelectric, dielectric and piezoelectric devices and for holographic data storage, frequency doubling, waveguide structures and solid-state lasers [1–3] thanks to its excellent electro-optical, photo-refractive and nonlinear optical properties [4–7]. LN particles are used as an ideal feed material for crystal growth [8] or for preparation of LN thin films [9]. Moreover, the catalytic capability of LN particles has been recently addressed [10].

LN particles are conventionally fabricated through solid-state reaction between $Nb_2O_5$ and $Li_2CO_3$, according to

$$Nb_2O_5 + Li_2CO_3 = 2LiNbO_3 + CO_2 \quad \Delta G^{o}_{1273\ K} = -149.0\ kJ \tag{1}$$

The solid-state reaction process, however, requires high temperatures ($>1000$ °C) to be carried out [11,12], and hence causes the evaporation losses of $Li_2O$, which may yield not only LN but also $Li_3NbO_4$ and $LiNb_3O_8$ components in the whole system [13]. The loss of stoichiometry by $Li_2O$ evaporation, together with the formation of Nb-rich grain boundaries deteriorates the piezoelectric properties of LN [14]. Therefore, development of a low-temperature processing method for the preparation of LN particles has attracted a great deal of attention. It was found that the synthesis temperature in the solid state mode can be reduced to below 600 °C by using a combustion agent such as urea [15–17] or glycine [18,19] and also by applying a ball milling pre-treatment [20,21]. In the later case, the ball-milling caused enhancement of the kinetics of the reaction by favouring the formation of more reactive surfaces. No further progress of these methods, however, has been reported.

Wet chemistry, as an alternative method for the synthesis of LN, makes it possible to employ a lower calcination temperature, avoiding losses of lithium oxide. In this category, the Pechini method is one in which the starting materials of citric acid, ethylene glycol as well as Nb and Li compounds are employed to prepare a gel, and LN is subsequently obtained by calcination of the gel at a temperature more than 560 °C [22]. Up to now, several works have been published based on this

---

*Corresponding author. Tel.: +44 1223 334315; fax: +44 1223 334567.
*E-mail addresses:* alirezakam@yahoo.com, ark42@cam.ac.uk (A.R. Kamali).

0272-8842/$ - see front matter © 2013 Elsevier Ltd and Techna Group S.r.l. All rights reserved.
http://dx.doi.org/10.1016/j.ceramint.2013.07.085

method for preparation of LN by using of $Nb_2O_5$ as the niobium source and $Li_2CO_3$ as the lithium source [23–26]. Apart from them, other materials such as $NbF_5$ [27], $NbCl_5$ [28], $Li_2C_2O_4$ [29], $LiNb(OPr^i)_6$ [30] and LiOH [31] have been employed as the source materials. In the wet chemistry methods, however, large amounts of expensive and mostly toxic organic compounds are required for synthesis of LN particles.

LN particles have also been synthesised via the hydrothermal method using different starting materials comprising of $LiOH \cdot H_2O$ (or $LiNO_3$) and $Nb_2O_5$ [32], LiOH and $Nb_2O_5 \cdot nH_2O$ [33], $Li_2CO_3$ and $Nb_2O_5$ [34] as well as LiOH and $Nb_2O_5$ [35]. Hydrothermal synthesis was found to be an efficient method in decreasing the synthesis temperature of LN to about 250 °C; however, the reaction time was very long, usually more than 10 h.

As a different approach, molten salt synthesis (MSS) has been used for the preparation of a large number of multi-component oxides from their precursors [36]. In order to prepare LN particles by this method, first, the Nb-source ($Nb_2O_5$ [37–39]) and the Li-source ($Li_2CO_3$ [38,39] or $LiOH \cdot H_2O$ [37]) were well mixed together with an appropriate salt mixture (KCl–NaCl [37–39] or $Li_2SO_4$–$Na_2SO_4$ [38]) by means of wet techniques. The mixed powders were then heated above the liquidus temperature of the salt mixture (over 600 °C). The main advantage of the MSS lies in the fact that the reaction between the reactants is facilitated due to the enhanced mobility of the species in the molten salt, which is $10^{10}$–$10^{13}$ times greater than that in the solid state [36]. As a consequence, the reaction can take place at a significantly reduced temperature and time. However, several hours are still required for the entire process to be completed, as the precursors should be mixed thoroughly before the heat-treatment.

In conclusion, the above mentioned processes are time consuming, expensive and/or complicated for mass-production of LN particles, and therefore more effective synthesis methods are required.

It should be noted that in the MSS approach the molten salt is used as the reaction medium and remains inert during the process. We have recently employed a molten salt synthesis approach [40,41], in which the salt can react with the other components during the process. This approach can be called the “reactive molten salt synthesis” (RMSS) in contrast with the common MSS approach. In the current study, for the first time, RMSS has been investigated as a method of preparing single-crystalline LN particles. The process consists of heating $Nb_2O_5$ powder in LiCl molten salt for a short period of time. The molten salt, therefore, is one of the precursors and is reactive.

## 2. Experimental procedure

### 2.1. Materials and methods

2.0 g $Nb_2O_5$ powder (208515, Sigma Aldrich) and 50.0 g LiCl (213233, Sigma-Aldrich) were mixed and the mixture was placed in an alumina crucible. Two sets of experiments

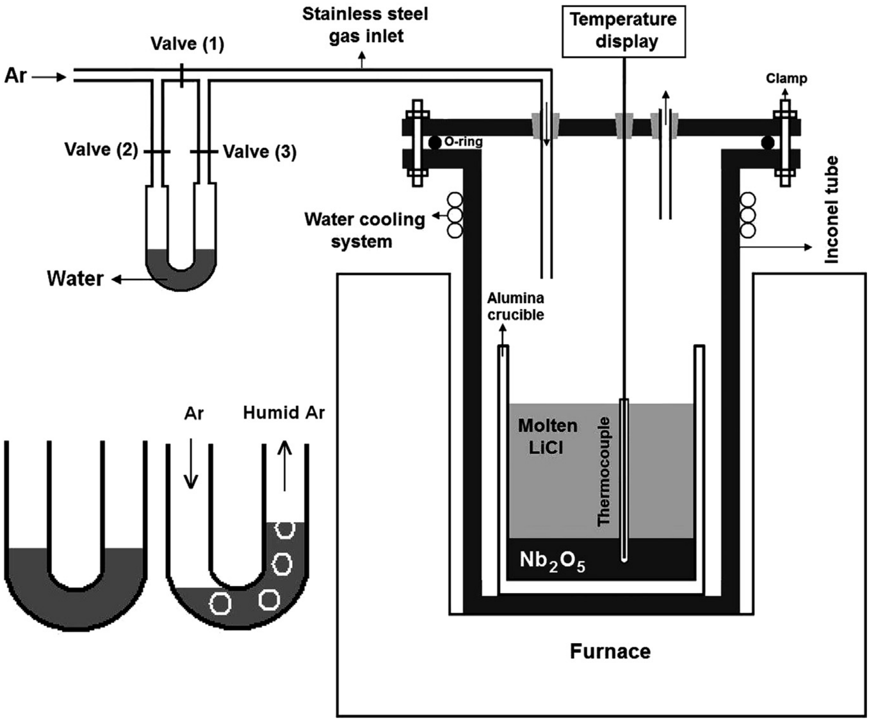

Fig. 1. A schematic representation of the experimental set-up used for the synthesis of LN. A mixture of $Nb_2O_5$ and LiCl was heated up to 700 °C under a flow of argon gas, while the valve (1) was open and the valves (2) and (3) were closed. At the target temperature, when the salt is in the molten state, a water containing atmosphere above the molten salt was provided by reversing state of the valves. In this situation, the Ar forms bubbles in the water bath to produce a humid gas stream (left bottom corner of the figure). Thereafter, the valves were switched into the initial state and the temperature was allowed to be reduced to the room temperature.

were conducted. In the first set, the crucible was placed in an electric furnace and heated to different temperatures ranging from 610 to 900 °C at a heating rate of 10 °C min$^{-1}$ under air. In the second set, the reactor of Fig. 1 was employed for heating the crucible. The reactor was a sealed Inconel vessel equipped with gas inlet and outlet, as schematised in Fig. 1. The gas inlet feed could be connected to a water bath and an argon cylinder, while the gas outlet to the exhaust system. Therefore, the reactor could be purged with humid argon flow when required. The crucible containing the mixture of LiCl–$Nb_2O_5$ was placed into the reactor at room temperature and heated under an argon flow of 40 cm$^3$ min$^{-1}$ to 700 °C, as indicated by the thermocouple placed inside the molten salt. The temperature difference between the furnace and the molten salt was 20 °C. When the target temperature was reached, the water bath was placed in the path of argon gas; and the humid gas was flowed over the crucible, as described in Fig. 1.

For all the experiments, the dwell time at the target temperature was 10 min. The crucible was then allowed to cool and the materials inside the crucible were rinsed with distilled water to remove the solidified LiCl and vacuum-filtered through filter paper (Whatman no. 100). The resulting powders were dried at 150 °C for 2 h.

### 2.2. Characterization

X-ray diffraction measurements were performed using a Philips PW 1710 X-ray diffractometer with Cu $K_\alpha$ radiation of wavelength 0.154 nm. The $2\theta$ step size was 0.05° and the dwell time per step was 25 s, and the patterns recorded were analysed using the X′Pert HighScore Plus software. The mean crystallite size ($L$) of the materials was calculated using Scherrer′s equation [42].

$$L = (0.9 \times 1.54)/(\mathrm{FWHM} \times \cos\theta) \qquad (2)$$

where FWHM is the full width at half maximum peak. The (001) peak of $Nb_2O_5$ and the (012) peak of LN were used for calculation of the mean crystallite size.

Micro-Raman spectroscopy was carried out using a Renishaw Ramanscope 1000 with a He–Ne ion laser of wavelength 633 nm. Curie temperature of the synthesised LN was measured using differential scanning calorimetry (SDT Q600, TA Instruments), in high-purity argon atmosphere at a heating rate of 20 °C min$^{-1}$. Morphological investigations were performed using a JEOL 6340F field emission scanning electron microscope (SEM) and a 200 kV FEI Tecnai F20 transmission electron microscope (TEM) equipped with selected area electron diffraction (SAED).

Thermodynamic data of selected reactions were calculated using a commercial software package [43].

## 3. Results and discussion

### 3.1. Characterisation of LiCl and $Nb_2O_5$ reactants

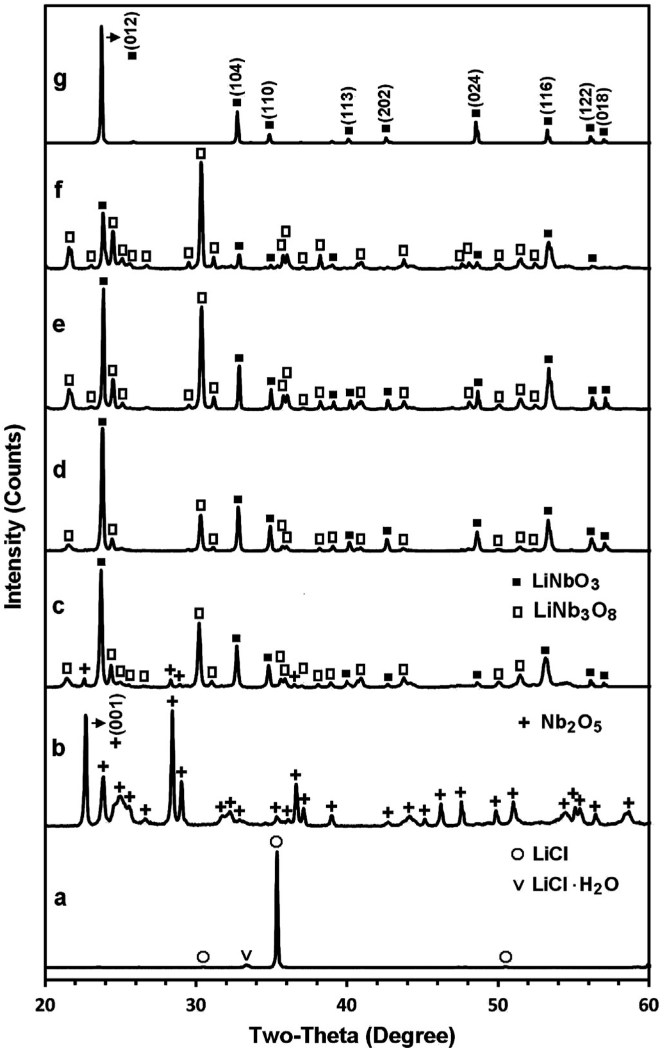

Fig. 2. XRD patterns of (a) LiCl, extracted from [44], and (b) the $Nb_2O_5$ starting materials. This figure also shows the XRD patterns of the product obtained by heating the LiCl–$Nb_2O_5$ mixture at (c) 610 °C, (d) 700 °C, (e) 800 °C and (f) 900 °C in air. (g) XRD pattern of the product obtained by heating the mixture in humid argon flow.

The XRD pattern of the as-received LiCl, extracted from our previous work [44], is presented in Fig. 2a. The XRD pattern indicates that anhydrous LiCl is the major component in the material, while a minor amount of monohydrate $LiCl \cdot H_2O$ is also available. It is known that LiCl can readily absorb water from the ambient atmosphere to form a surface layer of lithium chloride mono-hydrate [44]. The reactions during heating LiCl at the heating rate of 10 °C min$^{-1}$ under an ambient air flow has also been investigated [44]. It was found that LiCl is dehydrated below 200 °C, and the dehydrated LiCl melts at 608 °C. With further heating to 800 °C and above, the molten LiCl is hydrolysed by the moisture in the atmosphere to form oxide impurities in the molten salt, according to

$$2LiCl + H_2O(g) = Li_2O + 2HCl(g) \qquad (3)$$

The values of the standard Gibbs free energy change of reaction (3) as a function of temperature are shown in Fig. 3. It was further observed that the evaporation of molten salt is completed at 1032 °C which is far below the nominal boiling temperature of LiCl (1360 °C). It was attributed to the co-evaporation of lithium oxide and lithium chloride [44].

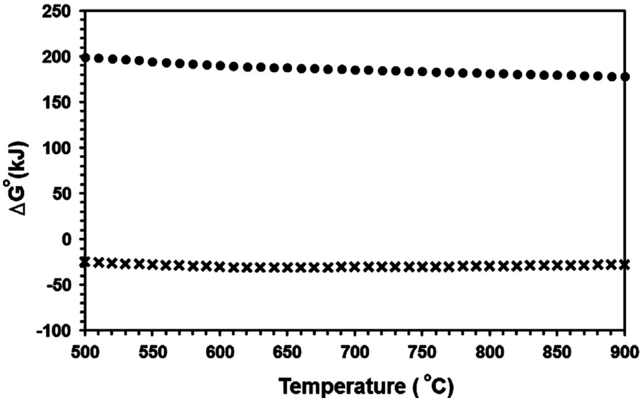

Fig. 3. The temperature variation of the change in the standard Gibbs free energy for reaction (3) (circles) and reaction (4) (crosses) calculated using [43].

Reaction (3) provides an insight into a way for synthesising metal-lithium-oxides. This approach is based on the reaction of metal oxides with newly formed lithium oxide in molten LiCl. The current study deals with the preparation of LN. Therefore, the reaction of $Nb_2O_5$ with the molten salt will be investigated in the following sections.

Fig. 2b shows the XRD pattern of the $Nb_2O_5$ reactant. It possesses orthorhombic symmetry (JCPDS 27-1003) with a mean crystallite size of 5 nm calculated using Eq. (2). The SEM micrograph of the material is shown in Fig. 4a. As seen, the $Nb_2O_5$ powder comprises of particles ranging in size between 200 nm to 500 nm. It is clear that each particle consists of fine grains less than 50 nm in size.

### 3.2. Heating the LiCl–$Nb_2O_5$ mixture in air

The LiCl–$Nb_2O_5$ mixture was heated in air atmosphere to different temperatures ranging from 610 to 900 °C for 10 min,

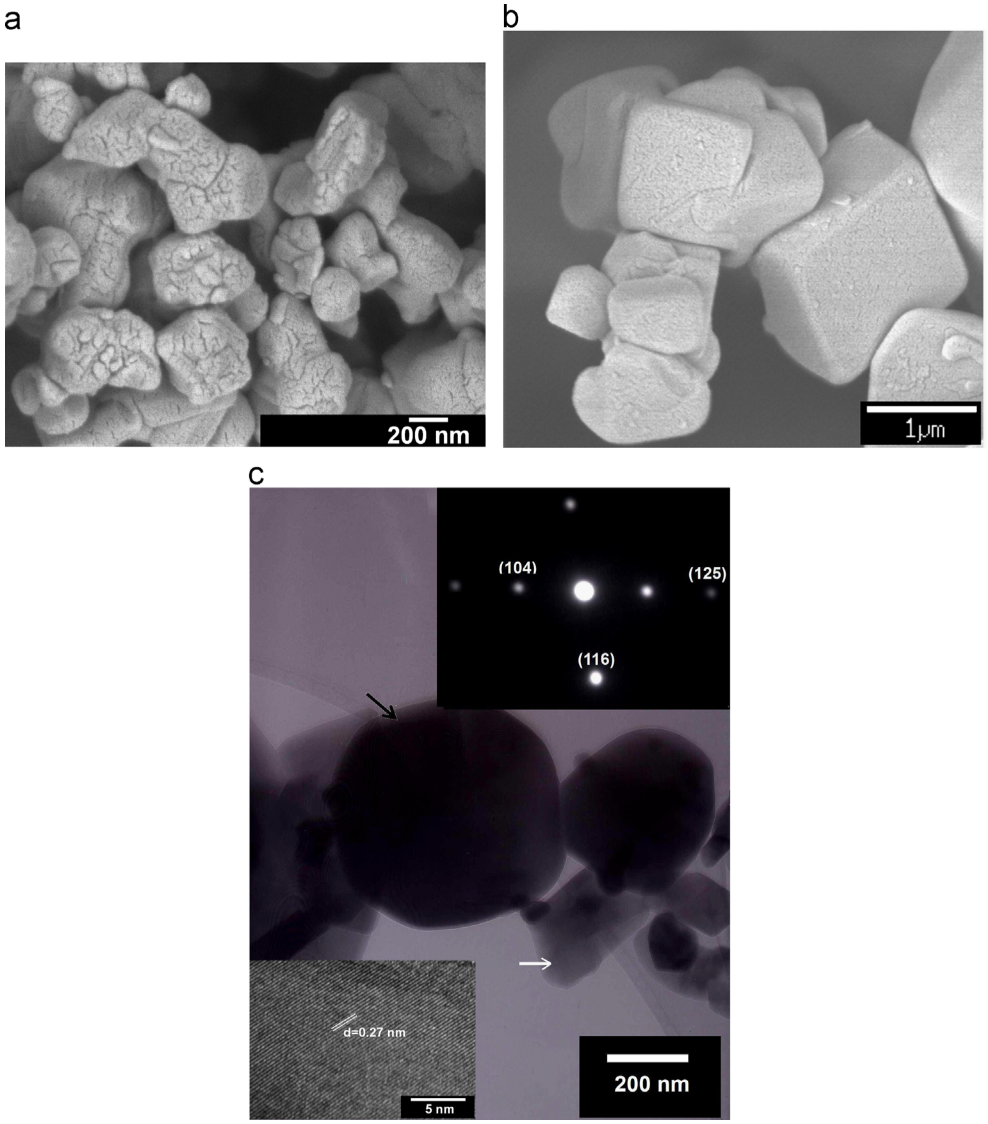

Fig. 4. (a) SEM morphology of $Nb_2O_5$ starting material as well as (b) SEM and (c) TEM bright-field image of synthesised LN particles. The upper inset in Fig. 4c is the SAED pattern taken from the crystal pointed by the black arrow. The lower inset is the high-resolution TEM micrograph of the area marked by the white arrow. It shows the lattice fringes with interplanar spacing of 0.27 nm, corresponding to the rhombohedral LN structure (104) planes.

and the XRD patterns of the products obtained are shown in Fig. 2c–f. Fig. 2c indicates that the product obtained at 610 °C contained LN with a rhombohedral symmetry (JCPDS 85-2456) as the major phase and $LiNb_3O_8$ with a monoclinic symmetry (JCPDS 36-0307) as the minor phase. A trace amount of un-reacted $Nb_2O_5$ is also visible in the product. This observation is remarkable as it suggests that LN can be synthesised by simple heating a mixture of $Nb_2O_5$ and LiCl. The formation of LN can be attributed to the occurrence of reaction (4), which takes place in the presence of humidity in the atmosphere.

$$Nb_2O_5 + 2LiCl + H_2O = 2LiNbO_3 + 2HCl \quad (4)$$

Fig. 3 shows the value of the standard Gibbs free energy change of reaction (4) as a function of temperature. Comparing these values with those calculated for reaction (3) leads to an interesting conclusion that although the standard free energy of formation of lithium oxide from lithium chloride, in the presence of water vapour (reaction (3)) is positive, the addition of niobium oxide to form lithium niobate allows the standard free energy for the formation to substantially reduce and become negative. Essentially, in this case, lithium oxide is only present as transient product.

Fig. 2d shows the XRD pattern of the product obtained by heating the LiCl–$Nb_2O_5$ mixture at 700 °C. As can be seen, the product again contained LN as the major and $LiNb_3O_8$ as the minor phases, while no peak related to $Nb_2O_5$ could be detected. With further increase of temperature from 700 to 800 °C, the relative intensity of the peaks of $LiNb_3O_8$ phase increases as observed in Fig. 2e. Finally, Fig. 2f indicates that a major phase of $LiNb_3O_8$ and a minority of LN will be obtained by increasing the temperature of the treatment to 900 °C.

In the system $Nb_2O_5$–$Li_2O$ [45], LN is the only stable phase at high $Li_2O$ content. Formation of $LiNb_3O_8$ phase, therefore, is associated with the loss of $Li_2O$ due to its volatility at high temperatures.

The reactivity in air of LiCl molten salt with $Nb_2O_5$ explained above provides the evidence for feasibility of the RMSS approach for the preparation of Li–Nb–O compounds. It is worth noting that the formation of the single phase LN can be promoted by raising the moisture content of the atmosphere, according to reaction (4). This idea will be explored in the following sections.

### 3.3. Heating the LiCl–$Nb_2O_5$ mixture in humid argon

The mixture of 2.0 g $Nb_2O_5$ and 50.0 g LiCl was heat-treated at 700 °C for 10 min in a humid argon flow by using the setup shown in Fig. 1. After cooling, rinsing and drying, a flame colour powder was obtained (3.2 g). Fig. 2g shows the XRD pattern of the product, from which one can deduce that the product is single-phase LN. The solution obtained from the rinsing process was heated at 130 °C overnight. After removal of the water by evaporation, LiCl (40 g) was recovered.

The result obtained demonstrates the completion of reaction (4) towards the formation of LN, and can be of academic and industrial interest.

The mean crystallite size of LN particles synthesised was calculated using Eq. (2). Accordingly, it can be concluded that the rapid molten salt heat treatment of the $Nb_2O_5$ powder with orthorhombic symmetry and the mean crystallite size of 5 nm leads to the formation of LN particles with rhombohedral crystal structure and the mean crystallite size of 56 nm.

The morphology of the LN synthesised is shown in Fig. 4. The SEM image presented in Fig. 4b reveals the presence of crystals with a size of several hundred nanometres. Moreover, micrometer-sized particles could also be observed through SEM analyses. Fig. 4c shows a TEM bright-field image of the synthesised LN particles; and the upper inset is the SAED pattern taken from the particle pointed by the black arrow in Fig. 4c, indicating that the particle is single-crystalline rhombohedral LN. The lower inset in Fig. 4c is a high-resolution TEM image recorded on the individual particle pointed by the white arrow, which shows the fringes of the LN (104) planes.

Taken together, Figs. 2 and 4 suggest the growth of LN crystals in the molten salt during the heat treatment of $Nb_2O_5$ powders under a water containing atmosphere, according to reaction (4). The reason why reaction (4) is much faster than the conventional solid-state reaction (1) lies in the fact that when the molten salt wets the $Nb_2O_5$ powders, an ideal connection on an atomic/ionic scale is made between the reactants. Therefore, the kinetic of the reaction will be high avoiding a need for prolonged high-temperature heat treatments.

Further experiments were carried out with different LiCl:$Nb_2O_5$ mole ratios ranging from 100:1 to 200:1, and the same results were obtained. This is due the fact that the LiCl:$Nb_2O_5$ ratios used were considerably higher than the ratio of 2:1 suggested by reaction (4).

### 3.4. DSC and Raman characterisation of the synthesised LN particles

It should be noted that while stoichiometric LN contents of 50 mol% $Li_2O$, the LN rhombohedral crystal structure can exist in variable $Li_2O$ contents of 46–50 mol% [46,47]. Therefore, further characterisation was performed to determine the chemical composition of our synthesised LN particles.

It is known that Curie temperature in LN is very sensitive to the chemical composition, according to the empirical Eq. (5) [48].

$$C_{Li} = 19.149 + 2.557 \times 10^{-2} T_c \quad (5)$$

where $C_{Li}$ is the crystal composition in mol% $Li_2O$, and $T_c$ is the Curie temperature.

DSC measurement was employed in order to evaluate the Curie temperature and therefore the composition of the sample. As shown in Fig. 5, the Curie temperature of the synthesised particles is 1164 °C, leading to calculate the $Li_2O$ content of the particles as 48.9 mol%.

Raman spectroscopy was used to investigate the vibrational characteristics of the synthesised LN crystals. The material at room temperature exhibited the Raman spectrum (Fig. 6) corresponding to the E(TO) and $A_1$(LO) modes of LN rhombohedral structure, with an additional peak at 608 $cm^{-1}$

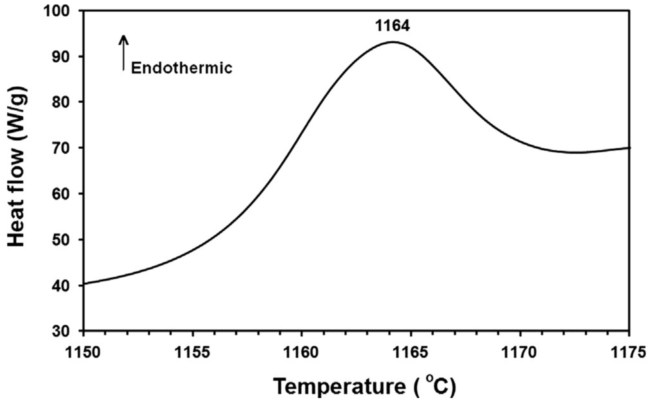

Fig. 5. DSC curve of the synthesised LN particles at a heating rate of 20 °C min$^{-1}$ showing an endothermic peak corresponding to the Curie temperature.

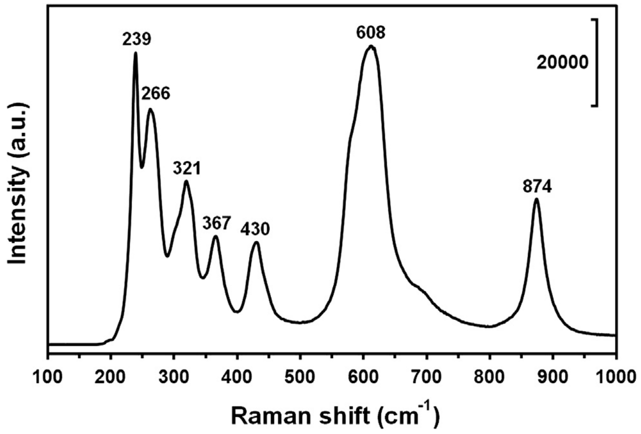

Fig. 6. Raman spectra of the synthesised LN particles at room temperature. Raman peaks at 239, 266, 321,367 and 430 cm$^{-1}$ correspond to E(TO) symmetry, and that at 874 cm$^{-1}$ is of A1(LO) symmetry. The strong peak at 608 cm$^{-1}$ might be induced by the lack of stoichiometries in the synthesised LN.

which might be induced by the lack of stoichiometries [49,50]. The Nb and Li vibrations in the E modes are confined to the ($xy$) plane, while those in the A modes to the ($z$) direction. These modes are sensitive to the stoichiometry of LN crystals, resulting in the shift and broadening of some Raman bands. $A_1$ mode at 874 cm$^{-1}$ can be used to estimate the chemical composition of the particles according to the empirical Eq. (6) [51].

$$C_{Li} = 53.29 - 0.1837 \times W \qquad (6)$$

where $W$ is the line width of the Raman peak. The line width of the 874 cm$^{-1}$ peak is measured to be 27.1 cm$^{-1}$. Therefore $C_{Li}$ is calculated to be 48.31 mol% which is in good agreement with the value obtained by the other method employed in this paper.

The results are consistent with the synthesis of non-stoichiometric LN particles. We believe the approach described here makes it possible to synthesise large amounts of not only LN but also a variety of other lithium-metal-oxides in a very short amount of time. Moreover, different chemical compositions and particle sizes of products may be obtained by careful control of the process parameters such as time and temperature.

## 4. Conclusions

The reactive molten salt synthesis method for the ultra-rapid preparation of single-crystalline LN particles was described. The method involves heating $Nb_2O_5$ powder in LiCl molten salt for a short time. Heating the LiCl–$Nb_2O_5$ mixture in air atmosphere led to the formation of different Li–Nb–O phases, while increasing the treatment temperature decreased the LN content of the product. In contrast, single-phase LN could be prepared by heating the mixture in a water-containing atmosphere at 700 °C. The process proceeds by the formation of solute $Li_2O$ via hydrolysis of LiCl, which subsequently reacts with $Nb_2O_5$ powder to form LN. The structure, morphology and chemical composition of the synthesised LN were characterised by different methods, which consequently showed the formation of non-stoichiometric pure-single crystalline LN particles. Proposed in this paper is a new way for the preparation of LN, in which the molten salt acts as both the reaction medium and the precursor.

## Acknowledgements

ARK would like to thank the Worshipful Company of Armourers and Brasiers for the financial support.

## References

[1] R.H. Kim, H.H. Park, G.T. Joo, The growth of $LiNbO_3$ (006) on MgO (001) and $LiTaO_3$ (012) substrates by sol–gel procedure, Applied Surface Science 169–170 (2001) 570–574.
[2] X.H. Zhen, X.J. Zhang, L.C. Zhao, Y.H. Xu, Growth and optical properties of In:Nd:$LiNbO_3$ crystals, Solid State Communications, 126, 203–205.
[3] D. Xue, K. Kitamura, Dielectric characterisation of the defect concentration in lithium niobate single crystals, Solid State Communications 122 (2002) 537–541.
[4] R.S. Weis, T.K. Gaylord, Lithium niobate: Summary of physical properties and crystal structure, Applied Physics A 37 (1985) 191–203.
[5] G.A. Magel, M.M. Fejer, R.L. Byer, Quasi-phase-matched second-harmonic generation of blue light in periodically poled $LiNbO_3$, Applied Physics Letters 56 (1990) 108–110.
[6] P. Baldi, M.P. De Micheli, K.E. Hadi, S. Nouh, A.C. Cino, P. Aschieri, D.B. Ostrowsky, Proton exchanged waveguides in $LiNbO_3$ and $LiTaO_3$ for integrated lasers and nonlinear frequency converters, Opical Engineering 37 (1998) 1193–1202.
[7] A.F. Benner, H.F. Jordan, V.P. Heuring, Digital optical computer with optically switched directional couplers, Opical Engineering 30 (1991) 1936–1941.
[8] S. Yao, F. Zheng, H. Liu, J. Wang, H. Zhang, T. Yan, J. Wu, Z. Xia, X. Qin, Synthesis of stoichiometric $LiNbO_3$ nanopowder through a wet chemical method, Crystal Research and Technology 44 (2009) 1235–1240.
[9] K. Wasa, M. Kitabatake, H. Adachi, Thin Film Materials Technology: Sputtering of Compound Materials, William Andrew, Inc.-Springer, USA, 2004.
[10] G. Pecchi, B. Cabrera, A. Buljan, E.J. Delgado, A.L. Gordon, R. Jimenez, Catalytic oxidation of soot over alkaline niobates, Journal of Alloys and Compounds 551 (2013) 255–261.
[11] G. Bhagavannarayana, R.V. Ananthamurthy, G.C. Budakoti, B. Kumar, K.S. Bartwal, A study of the effect of annealing on Fe-doped $LiNbO_3$ by HRXRD, XRT and FT-IR, Journal of Applied Crystallography 38 (2005) 768–771.

[12] F.Z. Fadil, M. Aillerie, T. Lamcharfi, F. Abdi, Synthesis and characterisation of holmium doped lithium niobate powders, Ceramics International 37 (2011) 2281–2285.

[13] V.T. Kalinnikov, O.G. Gromov, G.B. Kunshina, A.P. Kuzmin, E.P. Lokshin, V.I. Ivanenko, Preparation of $LiTaO_3$, $LiNbO_3$, and $NaNbO_3$ from peroxide solutions, Inorganic Materials 40 (2004) 411–414.

[14] L.B. Kong, T.S. Zhang, J. Ma, F. Boey, Progress in synthesis of ferroelectric ceramic materials via high-energy mechanochemical technique, Progress in Materials Science 53 (2008) 207–322.

[15] M. Liu, D. Xue, S. Zhang, H. Zhu, J. Wang, K. Kitamura, Chemical synthesis of stoichiometric lithium niobate powders, Materials Letters 59 (2005) 1095–1097.

[16] M. Liu, D. Xue, An efficient approach for the direct synthesis of lithium niobate powders, Solid State Ionics 177 (2006) 275–280.

[17] M. Liu, D. Xue, Effect of heating rate on the crystal composition of ferroelectric lithium niobate crystallites, Journal of Alloys and Compounds 427 (2007) 256–259.

[18] C.L. Kuo, Y.S. Chang, Y.H. Chang, W.S. Hwang, Synthesis of nanocrystalline lithium niobate powders via a fast chemical route, Ceramics International 37 (2011) 951–955.

[19] C.L. Kuo, G.J. Chen, Y.S. Chang, J.X. Fu, Y.H. Chang, W.S. Hwang, Thermal behavior of the nonstoichiometric lithium niobate powders synthesised via a combustion method, Ceramics International 38 (2012) 3729–3733.

[20] J.H. Luo, Preparation of lithium niobate powders by mechanochemical process, Applied Mechanics and Materials 121-126 (2012) 3401–3405.

[21] R.S. de Figueiredo, A. Messai, A.C. Hernandes, A.S.B. Sombra, Piezoelectric lithium niobate by mechanical alloying, Journal of Materials Science and Letters 17 (1998) 449–451.

[22] Y. Narendar, G.L. Messing, Mechanisms of phase separation in gel-based synthesis of multicomponent metal oxides, Catalysis Today 35 (1997) 247–268.

[23] J.P. Zhao, X.R. Liu, L.S. Qiang, Characteristics of the precursors and their thermal decomposition during the preparation of $LiNbO_3$ thin films by the Pechini method, Thin Solid Films 515 (2006) 1455–1460.

[24] A.Z. Simoes, M.A. Zaghete, B.D. Stojanovic, C.S. Riccardi, A. Ries, A.H. Gonzalez, J.A. Varela, $LiNbO_3$ thin films prepared through polymeric precursor method, Materials Letters 57 (2003) 2333–2339.

[25] V. Bouquet, E.R. Leite, E. Longo, J.A. Varela, M. Guilloux Viry, A. Perrin, Multi-layered $LiNbO_3$ films prepared by a polymeric precursor method, Journal of the European Ceramic Society 21 (2001) 1521–1524.

[26] E.R. Camargo, M. Kakihana, Low temperature synthesis of lithium niobate powders based on water-soluble niobium malato complexes, Solid State Ionics 151 (2002) 413–418.

[27] V. Samuel, A.B. Gaikwad, A.D. Jadhav, S.A. Mirji, V. Ravi, A novel technique to prepare $LiNbO_3$ at low temperature, Materials Letters 61 (2007) 765–766.

[28] E.R. Camargo, M. Kakihana, Chemical synthesis of lithium niobate powders ($LiNbO_3$) prepared from water-soluble DL-malic acid complexes, Chemistry of Materials 13 (2001) 1905–1909.

[29] K. Beck, H. Seyeda, U. Sulkowski, A. Rosenkranz, Niobium Compound, US Patent no.7241 911, 2007.

[30] B.D. Wood, V. Mocanu, B.D. Gates, Solution-phase synthesis of crystalline lithium niobate nanostructures, Advanced Materials 20 (2008) 4552–4556.

[31] M. Liu, D. Xue, C. Luo, Wet chemical synthesis of pure $LiNbO_3$ powders from simple niobium oxide $Nb_2O_5$, Journal of Alloys and Compounds 426 (2006) 118–122.

[32] J. Yu, X. Liu, Hydrothermal synthesis and characterisation of $LiNbO_3$ crystal, Materials Letters 61 (2007) 355–358.

[33] M.N. Liu, D.F. Xue, K. Li, Soft-chemistry synthesis of $LiNbO_3$ crystallites, Journal of Alloys and Compounds 449 (2008) 28–31.

[34] M. Liu, D. Xue, A solvothermal route to crystalline lithium niobate, Materials Letters 59 (2005) 2908–2910.

[35] C. An, K. Tang, C. Wang, G. Shen, Y. Jin, Y. Qian, Characterisation of $LiNbO_3$ nanocrystals prepared via a convenient hydrothermal route, Materials Research Bulletin 37 (2002) 1791–1796.

[36] T. Kimura, Molten Salt Synthesis of Ceramic Powders, in: C. Sikalidis (Ed.), Advances in Ceramics—Synthesis and Characterisation, Processing and Specific Applications, InTech, Croatia, 2011, pp. 75–100.

[37] R.H..Arendt, J.H.Rosolowski, Molten Salt Synthesis of Alkali Niobate Powders, US Patent no. 4234557, 1980.

[38] Y. Lin, H. Yang, J. Zhu, F. Wang, H. Luo, Low-temperature rapid synthesis of $LiNbO_3$ powder by molten salt methods, Materials and Manufacturing Process 23 (2008) 791–795.

[39] A.C. Santulli, H. Zhou, S. Berweger, M.B. Raschke, E. Sutter, S. S. Wong, Synthesis of single-crystalline one-dimensional $LiNbO_3$ nanowires, CrystEngCommunity 12 (2010) 2675–2678.

[40] A.R. Kamali, D.J. Fray, Solid phase growth of tin oxide nanostructures, Material Science and Engineering B 177 (2012) 819–825.

[41] A.R. Kamali, D.J. Fray, Molten salt corrosion of graphite as a possible way to make carbon nanostructures, Carbon 56 (2013) 121–131.

[42] J.I. Langford, A.J.C. Wilson, Scherrer after sixty years: a survey and some new results in the determination of crystallite size, Journal of Applied Crystallography 11 (1978) 102–113.

[43] A. Roine, HSC Chemistry for Windows, Version 6.0, Outokumpu Research Oy, Finland, 2002.

[44] A.R. Kamali, D.J. Fray, C. Schwandt, Thermokinetic characteristics of lithium chloride, Journal of Thermal Analysis and Calorimetry 104 (2011) 619–626.

[45] A. Reisman, F. Holtzberg, Heterogeneous equilibria in the systems $Li_2O$-, $Ag_2O$–$Nb_2O_3$ and oxide-models, Journal of the American Chemical Society 80 (1958) 6503–6507.

[46] H.M. Obryan, P.K. Gallagher, C.D. Brandle, Congruent Composition and Li-Rich Phase Boundary of $LiNbO_3$, Journal of the American Ceramic Society 68 (1985) 493–496.

[47] A. Weidenfelder, J. Shi, P. Fielitz, G. Borchardt, K.D. Becker, H. Fritze, Electrical and electromechanical properties of stoichiometric lithium niobate at high-temperatures, Solid State Ionics 225 (2012) 26–29.

[48] P.F. Bordui, R.G. Norwood, D.H. Jundt, M.M. Fejer, Preparation and characterisation of off-congruent lithium niobate crystals, Journal of Applied Physics 71 (1992) 875–879.

[49] R.F. Schaufele, M.J. Weber, Raman scattering by lithium niobate, Physical Review 152 (1966) 705–708.

[50] A. de Bernabé, C. Prieto, A. de Andrés, Effect of stoichiometry on the dynamic mechanical properties of. $LiNbO_3$, Journal of Applied Physics 79 (1996) 143–148.

[51] U. Schlarb, S. Klauer, M. Wesselmann, K. Betzler, M. Wiihlecke, Determination of the Li/Nb ratio in lithium niobate by means of birefringence and Raman measurements, Applied Physics A 56 (1993) 311–315.